Radiology

Incomplete Endograft Apposition to the Aortic Arch: Bird-Beak Configuration Increases Risk of Endoleak Formation after Thoracic Endovascular Aortic Repair[1]

Takuya Ueda, MD, PhD
Dominik Fleischmann, MD
Michael D. Dake, MD
Geoffrey D. Rubin, MD
Daniel Y. Sze, MD, PhD

Purpose: To determine the clinical importance of the bird-beak configuration after thoracic endovascular aortic repair (TEVAR).

Materials and Methods: The institutional review board approved this retrospective study and waived the requirement to obtain informed consent from patients. Sixty-four patients (40 men, 24 women; mean age, 64 years) who underwent TEVAR were evaluated. The treated diseases included dissection ($n = 29$), degenerative aneurysm ($n = 13$), acute traumatic transection ($n = 8$), pseudoaneurysm ($n = 4$), penetrating aortic ulcer ($n = 6$), intramural hematoma ($n = 2$), and mycotic aneurysm ($n = 2$). Bird-beak configuration, defined as the incomplete apposition of the proximal endograft with a wedge-shaped gap between the device and the aortic wall, was assessed with postprocedural CT angiography. The presence and length of the bird-beak configuration were compared with the formation of endoleaks and adverse clinical events.

Results: Endoleaks were detected in 26 (40%) of the 64 patients, including 14 with type Ia endoleak formation, one with type Ib endoleak formation, six with type II endoleak formation (from the left subclavian artery), two with type IIo endoleak formation (from other arteries), and three with type III endoleak formation. Bird-beak configuration was observed in 28 (44%) of 64 patients and correlated significantly with the risk of developing a type Ia or IIa endoleak ($P < .01$). Mean bird-beak length was significantly longer ($P < .01$) in patients with a type Ia or II endoleak (mean length, 14.3 and 13.9 mm, respectively) than in patients without endoleaks (mean length, 8.4 mm). Adverse events included early aortic-related death in three patients, additional treatment for endoleak in eight patients, and stent-graft collapse or infolding in six patients.

Conclusion: Detection of bird-beak configuration is helpful in the prediction of adverse clinical events after TEVAR.

© RSNA, 2010

Since the Food and Drug Administration approved the first commercially available stent-graft product in 2005 (1), thoracic endovascular aortic repair (TEVAR) has become widely accepted as a major option in the treatment of thoracic aortic diseases, including atherosclerotic aortic aneurysms, intramural hematomas, penetrating aortic ulcers, mycotic aneurysms, traumatic aortic transections, and aortic dissections (2–5). Although long-term results are still controversial, TEVAR has been proved safe and efficacious, with satisfactory short- and midterm (up to 5 years) results (6,7).

Successful TEVAR requires adequate stability at its proximal and distal landing zones to avoid stent-graft migration, collapse, or endoleak formation (5,8–10). Flat, straight, long, and cylindrical landing zones are ideal for stable deployment of the stent grafts (9,11). Although TEVAR of the descending thoracic aorta has yielded satisfactory results (12), the treatment of segments with landing areas involving a curve, short length, severe taper or flare, and luminal surface irregularity continues to be a technical challenge (13,14).

Anatomic complexities at the aortic arch are the most important reasons for early and late stent-graft treatment failure. Landing zones located near or proximal to the origin of the left subclavian artery are associated with a high risk of endoleak formation (13,15,16). Angulation and curvature at the aortic arch are also likely to be substantial risk factors for technical failure. Designs of current stent-grafts are relatively stiff with long segments, and they are unable to conform to highly angulated or curved arches. Some investigators have reported that the lack of apposition of the device to the aortic wall along the lesser curve results in the bird-beak configuration, which is the radiologic detection of a wedge-shaped gap between the undersurface of the stent graft and the aortic wall (17–19).

The purpose of our study was to assess the clinical importance of the bird-beak configuration after TEVAR to subsequent complications, such as the formation of endoleaks and adverse clinical events.

Materials and Methods

One author (M.D.D.) is a member of the endovascular medical advisory board of W. L. Gore & Associates (Flagstaff, Ariz). All other authors had control of data submitted for publication.

Patients

The institutional review board approved this retrospective study and waived the requirement to obtain the informed consent of patients. Between January 2000 and October 2008, 160 consecutive patients were prospectively enrolled in six different Food and Drug Administration–sponsored clinical trials in which the Thoracic Excluder or TAG stent-graft device (W. L. Gore & Associates) was tested. Of the 160 enrolled patients, we identified all patients in

whom stent-graft devices were deployed in the aortic arch. A total of 64 patients were included in this study (40 men, 24 women; mean age, 64 years; age range, 19–89 years).

The patients underwent TEVAR for the following diseases: acute aortic dissection (n = 19 [retrograde Stanford type A dissection, n = 2; Stanford type B dissection, n = 17]), subacute Stanford type B aortic dissection (n = 8), chronic Stanford type B dissection after surgical repair of acute Stanford type A dissection (n = 2), atherosclerotic aortic aneurysm (n = 13), posttraumatic or postanastomotic pseudoaneurysm (n = 4), acute traumatic transection (n = 8), giant penetrating aortic ulcer (n = 6), intramural hematoma (n = 2), and mycotic aneurysm (n = 2).

Computed Tomography Angiography Protocol

For our routine postprocedural follow-up protocol, all patients underwent postprocedural computed tomography (CT) angiography prior to hospital discharge and within 1 week after TEVAR, as well as follow-up CT angiography 1, 6, and 12 months after TEVAR. Patients then underwent CT angiography annually after stent-graft implantation.

CT angiography was performed with one of four multidetector CT scanners according to the date of the examination: We used a four-row multidetector CT scanner (Somatom Volume Zoom; Siemens Medical Systems, Forchheim,

Advances in Knowledge

- The presence of bird-beak configuration after thoracic endovascular aortic repair (TEVAR) for an aortic arch pathologic condition significantly correlated with the risk of type Ia or IIs endoleak formation.

- Longer bird-beak length increased the risk of type Ia or IIs endoleak formation, with bird-beak lengths of 10- and 14-mm corresponding to 50% and 80% risk, respectively, of type Ia or IIs endoleak formation.

- Twenty (30%) of 64 patients who experienced a type Ia or IIs endoleak after TEVAR for an aortic arch pathologic condition required additional treatment of the endoleak, and 17 (85%) of these 20 patients had bird-beak configuration.

Implication for Patient Care

- Patients with bird-beak configuration need strict long-term follow-up because of the high risk of endoleak formation and collapse.

Germany), two 16-row multidetector CT scanners (Somatom Sensation 16, Siemens Medical Solutions, Forchheim, Germany; Light Speed Ultra 16, GE Medical Systems, Milwaukee, Wis), and a 64-row multidetector CT scanner (Light-Speed VCT; GE Medical Systems).

All CT angiographic images were acquired with a section thickness of 2.5 mm (four-row multidetector CT), 0.75 mm (16-row multidetector CT), or 0.625 mm (64-row multidetector CT). Sections were reconstructed at 2.5-mm (four-row multidetector CT), 1.25-mm (16-row multidetector CT), or 1.0-mm (64-row multidetector CT) intervals. The x-ray tube potential was kept at a constant 120 kVp for all scans, and the tube current ranged from 226 to 440 mA. Multidetector CT scans were performed with a pitch that ranged from 1.25 to 1.5 and a gantry rotation time of 0.5 or 0.6 second. For 16- and 64-row multidetector CT, a retrospective electrocardiographic-gated acquisition technique was used throughout the cardiac cycle and was reconstructed into 10 phases (from 0% through 90% of the RR interval). Generally, reconstructed images at 70% of the RR interval were used for this study unless records required the use of a different interval.

A nonionic contrast medium with 300 mg of iodine per milliliter (four-row multidetector CT) or 350 mg of iodine per milliliter (16- and 64-row multidetector CT) was administered into the antecubital vein via a 20-gauge intravenous catheter with a power injector. The contrast medium was administrated at a rate of 4 mL/sec for the four-row multidetector CT scan and a rate of 5 mL/sec for the electrocardiographic-gated 16-row multidetector CT scans. For the 64-row electrocardiographic-gated multidetector CT scans, the contrast medium was administered via biphasic injection with an initial bolus injection at a rate of 4–6 mL/sec and followed by a subsequent injection at a slower flow rate of 3.2–4.8 mL/sec that was tailored to the body weight of the patient (20). The scan delay was determined with automated bolus triggering, and the total volume of contrast medium administered was determined as the product of the scan time plus 8 seconds multiplied by the injection rate. Delayed phase acquisition was performed 90 seconds after contrast medium injection.
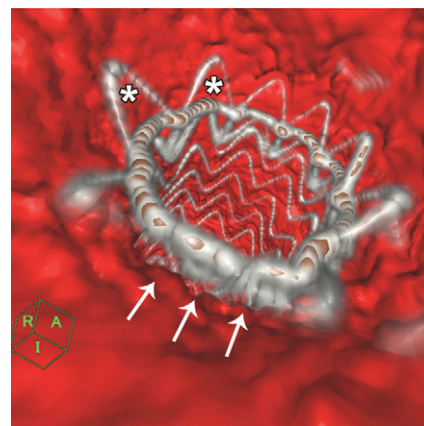
Bird-Beak Configuration

Postprocedural CT angiography in the arterial phase performed prior to hospital discharge was used to evaluate bird-beak configuration. A board-certified radiologist (T.U.) with 12 years of experience in cardiovascular radiology used a commercially available three-dimensional workstation (Aquarius-NET; TeraRecon, San Mateo, Calif) to interactively review CT angiographic images with three-dimensional volume-rendering reconstructions and thin-slab maximum intensity projections. Bird-beak configuration was defined as the lack of apposition of the proximal stent-graft to the aortic wall, with a wedge-shaped gap between the undersurface of the stent-graft and the aortic wall along the lesser curvature of the aortic arch (Fig 1). Three-dimensional reconstruction was performed interactively in real time, where slab thickness and obliquity of projection were optimized to enable the best orthogonal depiction of the bird-beak configuration.

Anatomic parameters were measured in each patient with a bird-beak configuration. Bird-beak length—the length of the longitudinal segment of the unapposed stent-graft—was measured with the three-dimensional workstation (Fig 1). The stent-graft devices are designed with scalloped flares of exoskeleton covered with fabric at the proximal and distal ends. These scalloped flares were excluded from length measurements. Bird-beak angle—the angle of the wedge-shaped gap between the undersurface of the stent-graft and the surface of the lesser curvature—was also measured with the three-dimensional workstation (Fig 1). In addition, the radiologist measured the longitudinal distance along the aortic center flow line from the origin of the left common carotid artery (LCCA) to the proximal end of the stent-graft (LCCA-stent distance) in all 64 patients. The radiologist also assessed whether the origin of the left subclavian artery (LSCA)
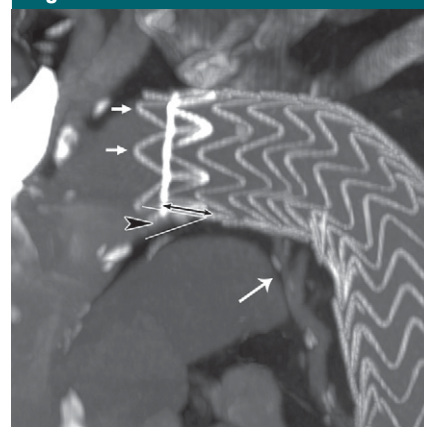
Figure 1

a.

b.

Figure 1: Images obtained in an 84-year-old woman who underwent TEVAR for an atherosclerotic aortic aneurysm show bird-beak configuration resulting in type Ia endoleak. **(a)** Thin-slab maximum intensity projection shows bird-beak configuration (arrowhead)—imperfect apposition at proximal end of stent-graft to lesser curve of aortic arch—resulting in wedge-shaped gap between undersurface of the stent-graft and aortic wall. Length (two-headed arrow) and angle of the bird-beak were measured with three-dimensional workstation functions. Scalloped flares (small arrows) at the proximal end of the device were excluded from measurement of bird-beak length. Leakage of contrast medium is observed flowing continuously from the bird-beak into the aneurysmal sac, signifying type Ia endoleak (large arrow). **(b)** Virtual angioscopic CT image shows proximal end of stent-graft, as viewed from ascending aorta. Proximal end of stent-graft is incompletely attached to aortic wall, resulting in a gap between the undersurface of the stent-graft and aortic lesser curve wall (arrows). Scalloped flares along greater curvature of device are well apposed to aortic wall (∗).

Table 1

Study Adaptation of Endovascular Abdominal Aortic Aneurysm Repair Endoleak Classification to TEVAR

Endoleak Type	Description
I	Leak occurring at proximal and/or distal attachment zones
Ia	Leak occurring at proximal landing zone
Ib	Leak occurring at distal landing zone
II	Leak caused by retrograde flow from covered vessels
IIs	Leak from left subclavian artery
IIo	Leak from bronchial or intercostal artery
III	Leak caused by structural endograft failure, such as inadequate seal between graft components or defect in the graft fabric
IV	Leak caused by graft fabric porosity
V	Aneurysmal sac growth caused by endotension without demonstrable endoleak

Figure 2

a.

b.

Figure 2: Images obtained in a 42-year-old man who underwent TEVAR for subacute type B aortic dissection show bird-beak configuration and developed a complex primarily type IIs endoleak. **(a)** Oblique sagittal thin-slab maximum intensity projection image shows enhancement of aortic false lumen (arrow), apparently fed by left subclavian artery (∗). Subsequent catheter angiography revealed small type Ia endoleak with anterograde flow from the aortic arch into the LSCA and retrograde flow in the aortic false lumen into the LSCA, which had to-and-fro flow. The dominant mechanism of endoleak was type IIs, as contrast enhancement in the left subclavian artery was almost the same as that in adjacent areas of endoleak, gradually fading away in the distal part, and false lumen near the proximal end of the stent graft was less enhanced than that in aortic true lumen. **(b)** Thicker-slab maximum intensity projection image shows bird-beak configuration (arrowhead). Stent-graft showed severe infolding at mid- and distal portions because of constraint of the device within narrow and tapered true lumen.

was covered by the stent-graft (LSCA coverage). A radiologist (T.U.) measured the bird-beak length and angle and the LCCA-stent distance for each patient three times and used the average.

Assessment of Endoleaks

The radiologist (T.U.) reviewed all available images obtained throughout the course of follow-up and confirmed the absence or presence of endoleak, as well as the type of endoleak (if any), by using delayed phase images. Endoleak assessment was performed independently, with a 10-day interval after the assessment of bird-beak configuration. The results of these retrospective assessments were obtained in a blinded fashion (relative to the original prospective reading and final patient disposition) and were compared with the original reports of the examinations in the patients' medical records. In the event of a discrepancy in interpretation between a retrospective assessment and the original report (endoleak presence vs absence, endoleak classification), the case was referred to a third radiologist (D.Y.S), who had 13 years of TEVAR experience and who settled the discrepancy with the radiologist who performed the retrospective assessment to reach a consensus.
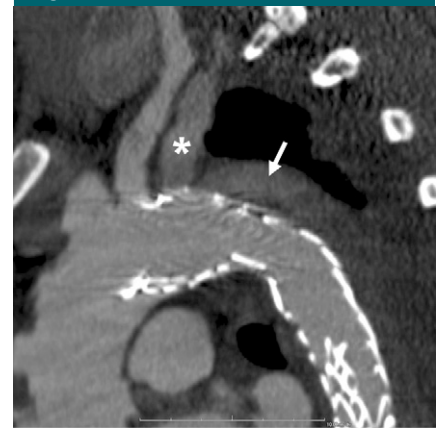
Table 1 describes our classification of endoleak types with a variation of the standard classification devised for endovascular abdominal aortic aneurysm repair (21,22). The definitions of type I, III, IV, and V endoleaks for endovascular abdominal aortic aneurysm

repair are applied to endoleaks for TEVAR without modification (22). As we hypothesized that a type II endoleak involving the left subclavian artery may be different from a type II endoleak involving other arteries because of the large diameter and close relationship to the aortic arch, we propose a subclassification for endoleaks that involve the left subclavian artery (type IIs) (Fig 2) and endoleaks that arise from other branch vessels, including the bronchial or intercostal arteries (type IIo). Among patients in whom multiple pathophysiologic mechanisms of endoleaks were detected, the disease was classified according to the dominant mechanism, which was decided by determining the direction of flow within the endoleak by measuring the direction of the gradient of contrast enhancement (Fig 2). Because of the small number of cases and the relevance of the endoleaks to the anatomic location of the bird-beak configuration, type Ib, IIo, III, IV, and V endoleaks were combined into a single group (hereafter, type other) for statistical analyses.
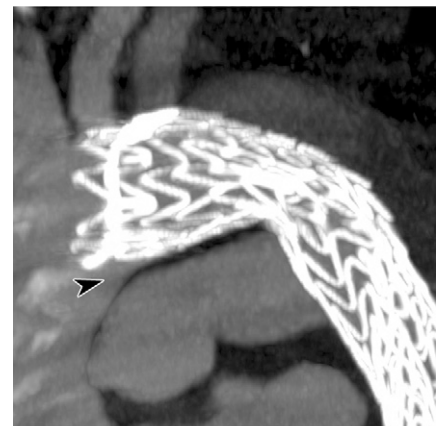
Adverse Events after TEVAR

A comprehensive survey of adverse events after TEVAR was performed by reviewing all hospital records, clinical trial records, and imaging studies. Aortic-related death within 12 months after TEVAR, endoleaks treated with surgical repair, additional stent-graft placement, interventional embolization of an endoleak, device collapse or infolding, and device migration were specifically targeted. The cause of any

Table 2

Endoleaks and Occurrence of Bird-Beak Configuration

Bird-Beak Configuration	Type of Endoleak						
	No leak	Ia	Ib	IIs	IIo	III	Total
Negative	28	1	1	2	2	2	36 (56)
Positive	10	13	0	4	0	1	28 (44)
Total	38 (59)	14 (22)	1 (2)	6 (9)	2 (3)	3 (5)	64 (100)

Note.—Data are numbers of patients. Data in parentheses are percentages.
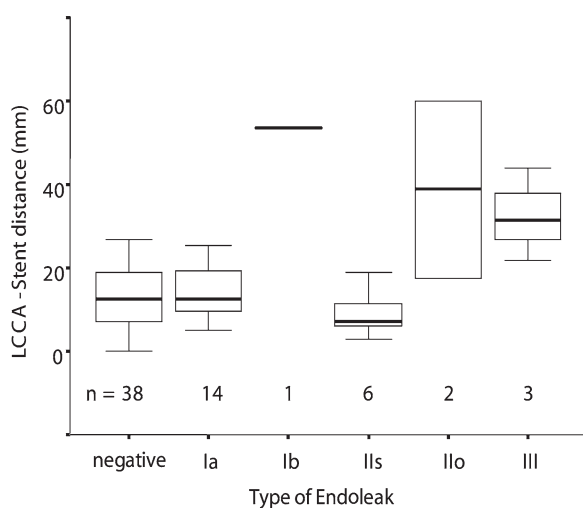
Figure 3

Figure 3: Distance from origin of left common carotid artery to proximal end of stent-graft (LCCA-stent distance) was grouped according to endoleak type. Box plots show distribution of LCCA-stent distance in each group. There was no significant difference between no-endoleak group *(negative)* and type Ia or IIs endoleak groups ($P = .22$, Kruskal-Wallis test). LCCA-stent distance in type Ib, IIo, and III endoleak groups tended to be longer than that in no-endoleak group; however, this difference was not significant ($P = .056$, Kruskal-Wallis test). Bottom and top of each box are lower and upper quartiles, respectively. Band in the middle of each box is median. Whiskers extending from bottom and top of each box are minimum and maximum values of group, respectively.

death was determined by reviewing death certificates and, when available, autopsy reports. Reinterventions (open surgical or endovascular) were also tallied, and the indications for reintervention were recorded.

Statistical Analysis

Statistical analysis was performed with commercially available statistical software (SPSS II for Windows, version 11; SPSS, Chicago, Ill). The relationship between the risk of endoleak formation and bird-beak configuration was assessed with a two-sided Fisher exact test. In the assessment of risk of endoleak formation, type Ia and IIs endoleaks were treated as a single group. The length and angle of the bird-beak were compared between the group with no endoleak and each endoleak group, including the type Ia, IIs, and other endoleak groups, by using the two-sample Mann-Whitney test. Statistical significance of LSCA coverage for the risk of endoleak formation was assessed with a two-sided Fischer exact test. The LCCA stent distance was compared between the group with no endoleak and each endoleak group by using the Kruskal-Wallis test. For all statistical analyses, $P < .05$ was considered to indicate a significant difference. The relationship between the risk of type Ia or IIs endoleaks and the length of the bird-beak was assessed with logistic regression analysis. In the logistic regression analysis, bird-beak length was determined by the presence of type Ia or IIs endoleaks, where the length of the bird-beak in patients who did not show bird-beak configuration was recorded as 0 mm, and those with type Ib, IIo, and III endoleaks were combined with the no endoleak group.

Results

Stent-grafts were successfully deployed in all patients. No immediate open surgical conversions were necessary. Intentional coverage of the LSCA was performed in 40 (62%) of 64 patients.

Endoleaks

Endoleaks were observed in 26 (40%) of 64 patients on the follow-up CT images throughout the follow-up course after TEVAR and included 14 type Ia endoleaks, one type Ib endoleak, six type IIs endoleaks, two type IIo endoleaks, and three type III endoleaks (Table 2). No patient in this study had a type IV or V endoleak. One patient had a delayed endoleak 12 months after TEVAR. Four patients had complex endoleaks that involved pathophysiology of both type Ia and IIs mechanisms. Of these patients, two had anterograde flow through the proximal perigraft space into the LSCA and the aortic false lumen; one patient had retrograde flow from the aortic false lumen into the LSCA through the proximal perigraft space, and one had retrograde flow from the LSCA into the aortic false lumen. All four patients with complex endoleaks underwent coverage of the LSCA.

Three cases yielded discrepancies in the assessment of endoleak classification. Type II endoleaks were not subclassified as type IIs or IIo endoleaks in the original clinical radiologic reports, and type IIs endoleaks had been underestimated and coded as type Ia endoleaks in three cases. After discussion with the third reviewer, two cases were finally coded as type IIs endoleaks with dominant flow from the LSCA, and one case was coded as predominantly type Ia with a complex endoleak of Ia and IIs. The patients with identified endoleaks were followed closely and were usually examined with follow-up CT angiography at 3-month (or shorter) intervals to monitor the increasing aortic diameter or other potential adverse sequelae.

Coverage of the LSCA was not significantly correlated with the risk of any type of endoleak in the cohort as a whole ($P = .177$). LCCA stent distances in all endoleak groups showed a trend that was not significantly different from
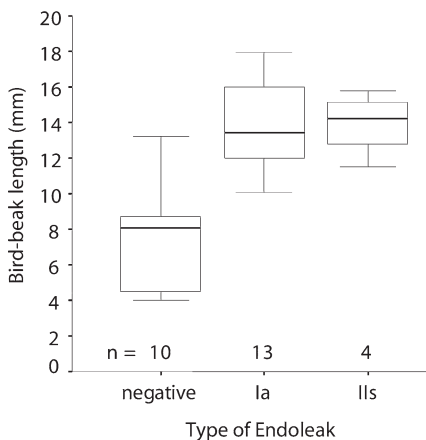
Radiology

Figure 4

Figure 4: Bird-beak length was compared between the no-endoleak group *(negative)* and type Ia or IIs endoleak groups. Box plots show a significant difference in bird-beak length between the no-endoleak group (mean, 8.4 mm ± 4.1) and type Ia (mean, 14.3 mm ± 2.1) and type IIs (mean, 13.9 mm ± 1.8) ($P <$ .01 and $P <$ .03, respectively; Mann-Whitney test) endoleak groups. See Figure 3 for a definition of the boxes and whiskers.

LCCA stent distances in the group with no endoleak ($P =$ .056) (Fig 3).

Bird-Beak Configuration

Bird-beak configuration was observed in 28 (44%) of 64 patients (Table 2). Thirteen (93%) of 14 type Ia endoleaks and four (67%) of six type IIs endoleaks were associated with bird-beak configuration. Type Ib and type IIo endoleaks were not associated with bird-beak configuration, and only one (33%) of three type III endoleaks was associated with bird-beak configuration. The presence of bird-beak configuration yielded a sensitivity of 74% (28 of 38 cases) and a specificity of 63% (18 of 26 cases) in the detection of any type of endoleaks and a sensitivity of 85% (17 of 20 cases) and a specificity of 75% (33 of 44 cases) in the detection of type Ia or IIs endoleak. The risk of type Ia or IIs endoleak formation was significantly correlated with the presence of a bird-beak configuration ($P <$ .01): Thirteen (93%) of the 14 patients with type Ia endoleaks and four (67%) of the six patients with type IIs endoleaks had positive findings for a bird-beak configuration (Table 2). Three (75%) of the four patients with
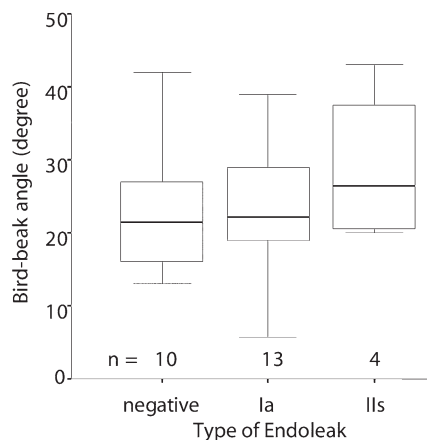
Figure 5

Figure 5: Bird-beak angle was compared between the no-endoleak group *(negative)* and type Ia or IIs endoleak groups. Box plots show no significant difference in bird-beak angle between the groups ($P =$ .64 for no-endoleak group vs type Ia endoleak group, $P =$ .61 for no-endoleak group vs type IIs endoleak group; Mann-Whitney test). See Figure 3 for a definition of the boxes and whiskers.

complex type Ia and IIs endoleaks had a bird-beak configuration. The risks for type Ib, IIo, and III endoleak formation were not significantly correlated with bird-beak configuration. The bird-beak length was significantly longer in the type Ia (mean, 14.3 mm ± 2.1 [standard deviation]) and type IIs (mean, 13.9 mm ± 1.8) endoleak groups than in the no-endoleak group (mean, 8.4 mm ± 4.1) ($P <$ .01 and $P <$ .03, respectively) (Fig 4). The bird-beak angle was not significantly different between the no-endoleak group (mean, 22.6° ± 9.3) and the type Ia endoleak group (mean, 25.6° ± 8.9) ($P =$ .64), nor was it significantly different between the no-endoleak group and the type IIs endoleak group (mean, 29.0° ± 10.1) ($P =$ .61) (Fig 5). When we compared the type Ia endoleak group with the type IIs endoleak group, there were no significant differences in length or angle of the bird-beak, LSCA coverage, or LCCA stent distance. Logistic regression analysis revealed that the risk of type Ia or IIs endoleaks increased as the length of the bird-beak increased: There was a 50% risk of endoleak at a bird-beak length of 9.5 mm and an 80% risk at a bird-beak length of 14 mm (Fig 6).

Adverse Events after TEVAR

Table 3 summarizes adverse events after TEVAR. Three patients died within 30 days after TEVAR. Two patients died of traumatic comorbidities, and one died of dissection-related multiorgan failure related to delayed diagnosis. None of the patients died of either aortic rupture or procedure-related complications. Eight additional patients died during mid-and long-term follow-up (2 months to 5 years); all deaths were confirmed to be unrelated to the original aortic diseases. Since all documented deaths were deemed unrelated to the stent-graft procedure and aortic disease, we concluded that mortality was not affected by the presence of bird-beak configuration.

Reinterventions for endoleaks were performed in eight patients, all of whom had large leaks and at least 5 mm of rapid (<12 months) or 8 mm of slow (>12 months) aortic false lumen or aneurysmal enlargement: Three patients underwent surgical transposition of the LSCA (type IIs endoleak, $n =$ 3); two patients underwent additional stent-graft placement for endoleaks (type Ia endoleak, $n =$ 1; type III endoleak, $n =$ 1); and three patients underwent embolization for endoleaks (type Ia endoleak, $n =$ 1; type Ib endoleak, $n =$ 1; type IIs endoleak, $n =$ 1). Six (30%) of the 20 patients with a type Ia or IIs endoleak underwent additional treatment after TEVAR, and five (83%) of the six patients showed signs of bird-beak configuration. Ten endoleaks resolved spontaneously without any additional treatment. Three endoleaks remained unchanged during follow-up without evidence of aneurysmal or false luminal enlargement and have not required any additional treatment. Five patients were either lost to follow-up or withdrew their consent and were not available for long-term follow-up.

Acute infolding or collapse of the stent-graft was observed in six patients. Four patients had collapse of the stent-graft in the proximal portion or midportion of the device, including one delayed collapse in a patient who underwent treatment for an anastomotic pseudoaneurysm. One patient had infolding in
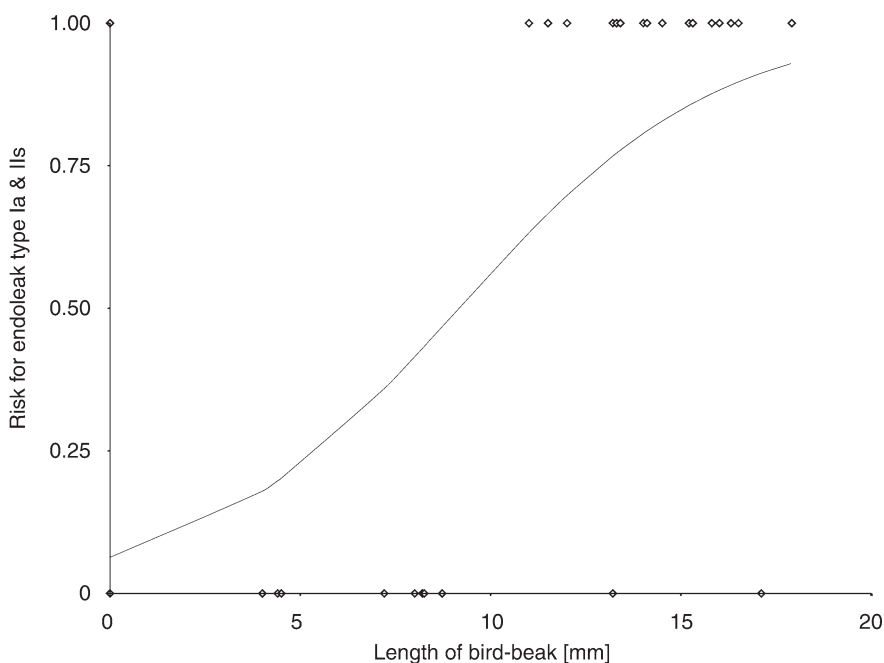
Radiology

Figure 6

Figure 6: The risk of type Ia or IIs endoleak formation was calculated with a fitted logistic regression curve according to length of bird-beak configuration. Curve shows that risk for type Ia or IIs endoleak increases as bird-beak length increases, reaching a risk of more than 50% at a length of 10 mm and a risk of more than 80% at a length of 15 mm. ◇ = observations.

Table 3

Summary of Adverse Postprocedural Events

Adverse Event	No. of Patients
30-day mortality	3 (No device- or procedure-related death)
Traumatic comorbidities	2
Multiorgan failure	1
Late death	8 (No aortic-related death)
Additional treatments for endoleaks	8
Surgical transposition of LSCA	3 (Two with type IIs endoleak that was positive for bird-beak configuration, one with type IIs endoleak that was negative for bird-beak configuration)
Additional stent-graft placement	2 (One patient had a type Ia endoleak that was positive for bird-beak configuration; one patient had a type III endoleak that was negative for bird-beak configuration)
Coil embolization	3 (One patient had a type Ia endoleak that was positive for bird-beak configuration; one patient had a type Ib endoleak that was negative for bird-beak configuration; one patient had a type IIs endoleak that was positive for bird-beak configuration)
Device collapse or infolding	6
Proximal and midportion	4 (All were positive for bird-beak configuration)
Midportion	1 (Negative for bird-beak configuration)
Distal portion	1 (Positive for bird-beak configuration)

the midportion of the device, and one had infolding in the distal portion of the device. Five (83%) of the six patients with infolding or collapse showed signs of bird-beak configuration. No patient showed signs of device migration.

Discussion

Our results show the clinical importance of bird-beak configuration after TEVAR and its association with adverse clinical events. The bird-beak configuration is significantly correlated with the risk of type Ia and IIs endoleak formation, and it is a potential risk factor for proximal stent-graft collapse or infolding. The unapposed lip of the stent-graft not only shortens the effective proximal landing zone, but it may also act as a baffle to direct pulsatile flow between the device and the aortic wall (10,11). Since patients who have major endoleaks—those with high flow, strong contrast enhancement, and frequently increasing aortic diameter during the course of follow-up—are subject to a high risk of rupture (23), aggressive endovascular or surgical reintervention may be indicated. Therefore, patients with bird-beak configuration need to undergo follow-up at closer intervals than prescribed by the routine postprocedural protocol, just like patients with major endoleaks.

Previous studies have largely dismissed type II endoleaks after TEVAR since they appear to occur less frequently after this procedure than they do after endovascular abdominal aortic aneurysm repair (24), and they are of questionable clinical importance in the abdomen (24,25). Our findings confirm that there are distinct differences in the outcome of type II endoleaks arising from the LSCA (type IIs endoleaks) and those arising from the bronchial and intercostal arteries (type IIo endoleaks). The LSCA is typically large in diameter and is a readily reversible source of collateral flow (9,11,26). In fact, one-third of patients with a type IIs endoleak required additional treatment, such as retrograde coil embolization after TEVAR due to continued false lumen or aneurysmal enlargement. As the use of TEVAR in the treatment of dissection increases, the complexity and clinical importance of type II endoleaks can no longer be dismissed.

Our study had some limitations. First, our study was performed in a retrospective manner. To reduce potential bias, the reader was blinded to patient information of complications at the evaluation

of bird-beak configuration, and the re-evaluated result for endoleaks was compared with the original radiologic report. Second, our study included only patients who were treated with a specific stent-graft device that performs somewhat differently from the Talent (Medtronic Vascular, Santa Rosa, Calif) and Zenith TX2 (Cook, Bloomington, Ind) devices. The risk of endoleak formation due to bird-beak configuration may be different for each device, as the differences in device designs—including stent segment lengths, longitudinal spines, fabric stiffness, and proximal fixation mechanism (covered flares, bare stent, barbs)—result in different shapes and degrees of apposition and sealing (19). Third, as anatomic parameters—including bird-beak length and angle and LCCA–stent distance—were measured by one person, the measurements may pose a potential error because of single-reader bias, even though the measurements were repeated and averaged to reduce the potential for error.

The problem of bird-beak configuration may influence the commercial design of next-generation devices, and the proof that imperfect apposition negatively affects clinical outcome makes this engineering pursuit particularly critical. Current cylindrical stent-graft products are designed to be used in the relatively straight descending thoracic aorta and are not optimized for use in the curved aortic arch (10,11,27). Next-generation devices are being tailored for the arch, with increased flexibility and conformability, preshaped curves, and/or branches to prevent bird-beak configuration and its associated risk for endoleak formation (10).

In summary, our results show the negative effect of bird-beak configuration on the clinical outcome after TEVAR and call for heightened awareness about bird-beak configuration with respect to preprocedural planning and postprocedural image interpretation and follow-up protocols.

References

1. Cho JS, Haider SE, Makaroun MS. US multicenter trials of endoprostheses for the endovascular treatment of descending thoracic aneurysms. J Vasc Surg 2006; 43(suppl A):12A–19A.

2. Nienaber CA, Fattori R, Lund G, et al. Nonsurgical reconstruction of thoracic aortic dissection by stent-graft placement. N Engl J Med 1999;340(20):1539–1545.

3. Greenberg RK, O'Neill S, Walker E, et al. Endovascular repair of thoracic aortic lesions with the Zenith TX1 and TX2 thoracic grafts: intermediate-term results. J Vasc Surg 2005;41(4):589–596.

4. Chu MW, Forbes TL, Kirk Lawlor D, Harris KA, Derose G. Endovascular repair of thoracic aortic disease: early and midterm experience. Vasc Endovascular Surg 2007;41(3):186–191.

5. Svensson LG, Kouchoukos NT, Miller DC, et al. Expert consensus document on the treatment of descending thoracic aortic disease using endovascular stent-grafts. Ann Thorac Surg 2008;85(1 suppl):S1–S41.

6. Demers P, Miller DC, Mitchell RS, et al. Midterm results of endovascular repair of descending thoracic aortic aneurysms with first-generation stent grafts. J Thorac Cardiovasc Surg 2004;127(3):664–673.

7. Verhoye JP, Miller DC, Sze D, Dake MD, Mitchell RS. Complicated acute type B aortic dissection: midterm results of emergency endovascular stent-grafting. J Thorac Cardiovasc Surg 2008;136(2):424–430.

8. Garzón G, Fernández-Velilla M, Martí M, Acitores I, Ybáñez F, Riera L. Endovascular stent-graft treatment of thoracic aortic disease. RadioGraphics 2005;25(1 suppl):S229–S244.

9. Ueda T, Fleischmann D, Rubin GD, Dake MD, Sze DY. Imaging of the thoracic aorta before and after stent-graft repair of aneurysms and dissections. Semin Thorac Cardiovasc Surg 2008;20(4):348–357.

10. Sze DY, Mitchell RS, Miller DC, et al. Infolding and collapse of thoracic endoprostheses: manifestations and treatment options. J Thorac Cardiovasc Surg 2009;138(2):324–333.

11. Sze DY, van den Bosch MA, Dake MD, et al. Factors portending endoleak formation after thoracic aortic stent-graft repair of aortic dissection. Circ Cardiovasc Interv 2009;2(2):105–112.

12. Mitchell RS, Miller DC, Dake MD. Stent-graft repair of thoracic aortic aneurysms. Semin Vasc Surg 1997;10(4):257–271.

13. Ishimaru S. Endografting of the aortic arch. J Endovasc Ther 2004;11(suppl 2):II62–II71.

14. Serag AR, Bergeron P, Mathieu X, Piret V, Petrosyan A, Gay J. Identification of proximal landing zone limit for proper deployment of aortic arch stentgraft after supra-aortic great vessels transposition. J Cardiovasc Surg (Torino) 2007;48(6):805–807.

15. Tse LW, MacKenzie KS, Montreuil B, Obrand DI, Steinmetz OK. The proximal landing zone in endovascular repair of the thoracic aorta. Ann Vasc Surg 2004;18(2):178–185.

16. Melissano G, Civilini E, Bertoglio L, et al. Results of endografting of the aortic arch in different landing zones. Eur J Vasc Endovasc Surg 2007;33(5):561–566.

17. Fayad A. Thoracic endovascular stent graft with a bird's beak sign. Can J Anaesth 2008;55(11):785–786.

18. Kölbel T, Lee T, Ivancev K, Resch TA, Sonesson B, Malina M. In situ bending of a thoracic stent-graft: a proposed novel technique to improve thoracic endograft seal. J Endovasc Ther 2008;15(1):62–66.

19. Canaud L, Alric P, Laurent M, et al. Proximal fixation of thoracic stent-grafts as a function of oversizing and increasing aortic arch angulation in human cadaveric aortas. J Endovasc Ther 2008;15(3):326–334.

20. Fleischmann D. How to design injection protocols for multiple detector-row CT angiography (MDCTA). Eur Radiol 2005;15(suppl 5):E60–E65.

21. Veith FJ, Baum RA, Ohki T, et al. Nature and significance of endoleaks and endotension: summary of opinions expressed at an international conference. J Vasc Surg 2002;35(5):1029–1035.

22. Parmer SS, Carpenter JP, Stavropoulos SW, et al. Endoleaks after endovascular repair of thoracic aortic aneurysms. J Vasc Surg 2006;44(3):447–452.

23. Criado FJ, Clark NS, Barnatan MF. Stent graft repair in the aortic arch and descending thoracic aorta: a 4-year experience. J Vasc Surg 2002;36(6):1121–1128.

24. Tolia AJ, Landis R, Lamparello P, Rosen R, Macari M. Type II endoleaks after endovascular repair of abdominal aortic aneurysms: natural history. Radiology 2005;235(2):683–686.

25. Jonker FH, Aruny J, Muhs BE. Management of type II endoleaks: preoperative versus postoperative versus expectant management. Semin Vasc Surg 2009;22(3):165–171.

26. Peterson MD, Wheatley GH 3rd, Kpodonu J, et al. Treatment of type II endoleaks associated with left subclavian artery coverage during thoracic aortic stent grafting. J Thorac Cardiovasc Surg 2008;136(5):1193–1199.

27. Nienaber CA, Kische S, Ince H. Thoracic aortic stent-graft devices: problems, failure modes, and applicability. Semin Vasc Surg 2007;20(2):81–89.